ELSEVIER

15 August 1999

Optics Communications 167 (1999) 183–189

OPTICS COMMUNICATIONS

www.elsevier.com/locate/optcom

Full length article

Surface plasmon propagation near an index step

Charles E.H. Berger [1], Rob P.H. Kooyman [*], Jan Greve

Department of Applied Physics, MESA Institute, Applied Optics Group, University of Twente, P.O. Box 217, 7500 AE Enschede, The Netherlands

Received 23 February 1999; received in revised form 24 May 1999; accepted 9 June 1999

Abstract

Propagation effects of surface plasmons on the surface plasmon microscopy (SPM) image of an area around the edge of a cover layer were studied as a function of the wavelength. A phenomenological model that describes these effects of surface plasmon propagation on the observed reflectance is presented. Theoretical and experimental results for wavelengths ranging from 560 to 660 nm for a 50 nm silver layer with 30 nm thick SiO_2 pattern on top were compared and found to agree quite well. © 1999 Elsevier Science B.V. All rights reserved.

Keywords: Surface plasmon; Plasmon propagation; Surface plasmon microscopy

1. Introduction

Generally, the application of Fresnel theory to the description of reflectometric measurements is straightforward and gives accurate results. In this work we will study propagation effects of surface plasmons on the surface plasmon microscopy (SPM) image of an area around the edge of a cover layer. Far from this index step Fresnel theory still applies, but at distances smaller than the propagation length of SPs (typically μm) it can no longer be used. Because Fresnel theory assumes that the layer system consists of layers without lateral structure, it can only provide the reflectance far from the step as a boundary condition.

We present a phenomenological model (based on that of Rothenhäusler and Knoll [1,2]) that describes the effect of plasmon propagation on the observed reflectance near an index step, and study this effect as a function of the wavelength. Silver layers were first characterized by fitting experimental SPR angular reflectance curves. Then, the model was used to predict the resulting reflectance profile when an index step on the metal layer was imaged with a surface plasmon microscope. Measurements and calculations were performed for wavelengths ranging from 560 to 660 nm for a 50 nm silver layer with a 30 nm thick SiO_2 pattern on top. Theoretical and experimental results were compared and found to agree quite well.

* Corresponding author. Correspondence address: Department of Applied Physics, Bio-interface Group, University of Twente, P.O. Box 217, 7500 AE Enschede, The Netherlands; tel.: +31-53-4893157; fax: +31-53-4891105; e-mail: r.p.h.kooyman@tn.utwente.nl

[1] Université de Bordeaux I, CPMOH, 351 Cours de la libération, 33405 Talence cedex, France. Tel.: +33-5-57962528; fax: +33-5-56846970; e-mail: charles.berger@iname.com

0030-4018/99/$ - see front matter
PII: S0030-4018(99)00309-0

2. Theory

In the following, κ is the x component of the wave vector, and may be complex ($\kappa = \kappa' + i\kappa''$). When a resonant plasmon with wave vector κ_0 propagates along x from an uncovered area into a covered area, a decaying plasmon (containing an imaginary component) with wave vector κ_1 results (see Fig. 1) [3]. Here, κ_1 is the wave vector for resonant excitation of the covered area. In addition to this transmitted wave, the external light source non-resonantly excites a wave with wave vector κ_0. The change of the surface plasmon electric field amplitude is governed by the imaginary part of its wave vector. The constants E_1 and E_2 are the resonant and the non-resonant plasmon amplitude, respectively. Leaving out the time dependence, the plasmon electric field at the interface is [1,2],

$$E_{\mathrm{pl}}(x) = (E_1 - E_2)e^{i(\kappa_1' + i\kappa_1'')x} + E_2 e^{i\kappa_0' x}, \qquad (1)$$

for $x \geq 0$, with $x = 0$ at the index step. We improved this model to predict the reflectance near the index step. Far from the index step, the assumptions of plane waves and infinite layers are valid, and if the boundary conditions are to be fulfilled the reflectance at a large distance from the step should coincide with Fresnel values. By imposing these conditions all parameters of the model are fixed.

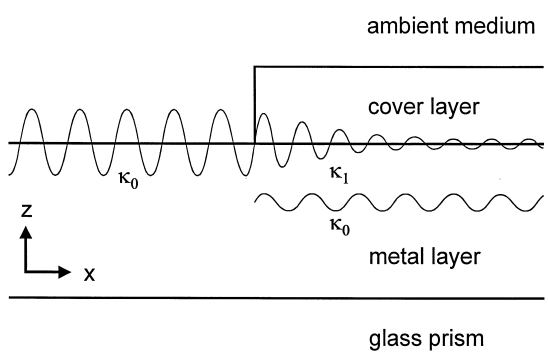

Fig. 1. Schematic representation of a surface plasmon with wave vector κ_0 propagating along a metal–air interface into a cover layer, where an exponentially decaying κ_1 plasmon results. The non-resonantly excited surface plasmon with wave vector κ_0 is indicated separately.

In Refs. [1,2] it is assumed that the non-resonant contribution to E_{pl} is constant and starting at $x = 0$. What is missing in this model is the fact that the plasmon electric field interferes with the incoming field from the light source. Because of this omission the model can give incorrect results, with a higher reflectance at resonance than off resonance. Therefore, for the total electric field reaching the detector an extra term should be introduced to account for the low reflectance resulting from resonant plasmon excitation, due to destructive interference [4]:

$$E_{\mathrm{tot}}(x) = (E_1 - E_2)e^{i(\kappa_1' + i\kappa_1'')x} + E_2 e^{i\kappa_0' x} - E_3 e^{i\kappa_0' x}, \qquad (2)$$

where E_3 is the amplitude of the incoming field. With $A = E_1 - E_2$ and $B = E_2 - E_3$, the resulting intensity can be written as

$$I_{\mathrm{tot}}(x) = |E_{\mathrm{tot}}(x)|^2 = B^2 + A^2 e^{-2\kappa_1'' x} + 2AB e^{-\kappa_1'' x}\cos(\kappa_1' - \kappa_0')x. \qquad (3)$$

For $x = -\infty$ (or $x \leq 0$) and $x = +\infty$, the intensity equals $(E_1 - E_3)^2$ and $(E_2 - E_3)^2$, respectively. We can solve these constants putting E_3 equal to 1 ($E_3 > E_1 > E_2 > 0$), because then $I_{\mathrm{tot}}(-\infty)$ and $I_{\mathrm{tot}}(+\infty)$ equal the macroscopic reflectance for uncovered and covered areas that can be calculated with Fresnel theory. Note that there are no free parameters to fit measurements.

When a non-resonant plasmon exits a covered area and becomes resonant the total electric field and intensity may be written in a similar way:

$$E_{\mathrm{tot}}(x) = E_2 e^{i\kappa_0' x} + (E_1 - E_2)(1 - e^{-\kappa_0'' x})e^{i\kappa_0' x} - E_3 e^{i\kappa_0' x}, \qquad (4)$$

and

$$I_{\mathrm{tot}}(x) = \left[B + A(1 - e^{-\kappa_0'' x})\right]^2, \qquad (5)$$

where the same definitions are used for the constants. The plasmon wave vectors were calculated using the position and half-width of the reflectance minimum [4] and depend on the properties of the metal layer and the cover layer.

3. Experimental section

3.1. Set-up

Two cavity-dumped dye lasers (3.8 MHz, Coherent 700) synchronously pumped by a mode-locked Nd:YLF laser (Antares 76-YLF, Coherent) served as a light source covering the wavelength range from 560 to 660 nm. The polarization could be modulated between *p*- and *s*-polarization electronically, using a Pockels cell (PC 100/4; Electro Optic Developments, Basildon, England). A rotation table (Micro-Controle UR80PP; angular increments: 1 mdeg.) was used for computer controlled reflectance scans that were measured with a photodiode.

The experimental set-up for the surface-plasmon microscope has previously been described in detail in Ref. [5]. It images the attenuated total reflectance in the Kretschmann configuration, and uses *p*- and *s*-polarized light to correct for inhomogeneities in the expanded incoming laser beam. A $7\times$ (NA 0.19) objective was used to image the light on a video camera (VCM 3250; Philips) which has an output that is linear in light intensity.

3.2. Sample preparation

Microscope glass slides were used as substrates on which a 50 nm silver layer was evaporated (1 nm/s at 10^{-6} mbar). After the evaporation, a photoresist layer was spun on the substrate and a pattern was made photolithographically. A 30 nm thick SiO_2 layer was sputtered (0.1 nm/s at 10^{-2} mbar Ar) over the bare and covered areas of the silver layer. After the removal of the photoresist using an ultrasonic acetone bath, a SiO_2 pattern on the silver resulted. Using this lift-off technique results in steep edges of better than 1 μm. Substrates were stored in a nitrogen atmosphere. They were attached to the prism (BK7 glass, 45°) using a matching oil.

4. Results and discussion

4.1. Substrate characterization

All measurements were carried out for wavelengths ranging from 560 to 660 nm in steps of 10 nm. First, the SPR reflectance of the bare silver layer was measured as a function of the angle of incidence. The low frequency part of the laser noise was effectively suppressed by measuring the reflectance switching the polarization between *p* and *s*, while integrating both signals. The ratio of the *p*- and *s*-reflectance as a function of the angle of incidence and the wavelength is displayed in Fig. 2. These normalized values can be directly compared to Fresnel calculations, taking into account the different transmission of the prism entrance and exit surfaces for different polarizations. The ratio of the transmissions of the prism for *p*- and *s*-polarized light is given by

$$\frac{T_p}{T_s} = \left(\frac{n_1 \cos\theta_1 + n_2 \cos\theta_2}{n_1 \cos\theta_2 + n_2 \cos\theta_1} \right)^4, \tag{6}$$

where θ_1 and θ_2 are the external and internal angles of the propagating light beam with respect to the normal of the entrance and exit surface, and n_1 and n_2 are the refractive index of the ambient medium and the prism, respectively. Fresnel formulae were used to fit the measured reflectance curves by varying the real and imaginary part of the dielectric constant ε and the thickness d of the silver layer. It has previously been demonstrated [6,7] that the reflectance curves depend on these three parameters in

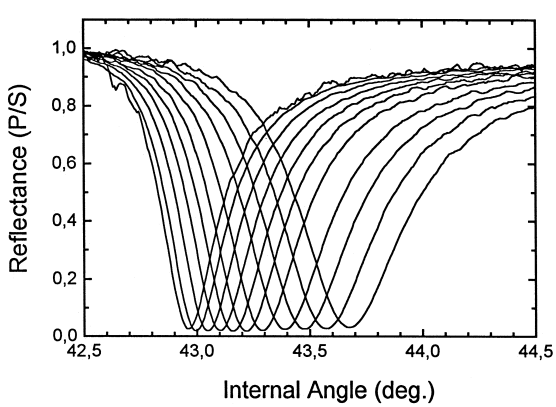

Fig. 2. Ratio of the reflectance for *p* and *s* polarized light as a function of the internal incident angle and wavelength (560–660 nm) for a 50 nm silver layer. Table 1 shows the results from fitting these measurements. For decreasing wavelength, the curves shift to higher angle values.

Table 1
Dielectric constant and thickness of the silver layer as a function of wavelength.

λ (nm)	ε_r	ε_i	d (nm)
560	−11.43	0.480	50.36
570	−11.97	0.502	50.41
580	−12.52	0.519	50.42
590	−13.08	0.536	50.49
600	−13.95	0.554	50.21
610	−14.53	0.578	50.23
620	−15.06	0.594	50.34
630	−15.62	0.602	50.30
640	−16.19	0.614	50.35
650	−16.80	0.629	50.22
660	−17.15	0.608	50.27

such a way that they can be determined separately. A computer program that was written (based on differential correction and the least squares criterion) needed less than 10 iterations to converge to the values presented in Table 1.

Of course d should not depend on the wavelength and indeed for the independent measurements at different wavelengths the same value for the layer thickness was found with a high accuracy (50.3 ± 0.1 nm). The excellent agreement of Fresnel calculation and experimental data can also be seen in Fig. 3, where a typical measurement is shown together with the calculated values as an example.

The thickness of the SiO_2 pattern on top of the silver layer was checked with a surface profiler (Dektak) and was indeed about 30 nm (see Fig. 4). The steepness of the edge was obscured by the tip convolution, but the lift-off method (as described in Section 3.2) produces edges narrower than 1 μm, which is sufficient for our purposes.

4.2. Reflectance near the index step

With the silver layer parameters ($\varepsilon_r, \varepsilon_i, d$) known, the reflectance profile near the index step can be calculated using the model that was presented in Section 2. The parameters in Eq. (3) can be derived from Fresnel calculations using ε and d. The constants A and B follow from the boundary condition that the reflectance far from the index step [$I_{tot}(-\infty)$ and $I_{tot}(+\infty)$] should equal to that given by Fresnel theory. The real part of the wave vectors κ_1 and κ_0 (corresponding to resonant SP excitation of covered and uncovered areas, respectively) can be determined from the position of the minimum in calculated angular reflectance curves. Finally, the imaginary part of the wave vectors κ_1 and κ_0 can be determined from the half-width of the SPR reflectance minimum [4].

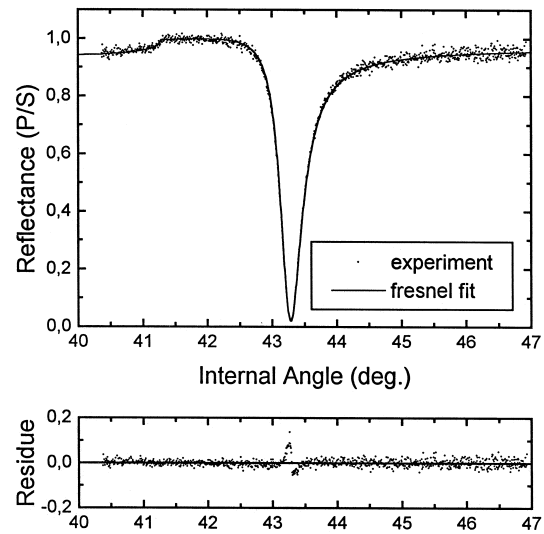

Fig. 3. Ratio of the reflectance for p- and s-polarized light as a function of the internal incident angle for wavelength $\lambda = 600$ nm, together with Fresnel fit ($\varepsilon = -13.95 + i0.554$ and $d = 50.2$ nm). The residue was calculated as the relative difference of theoretical and experimental values.

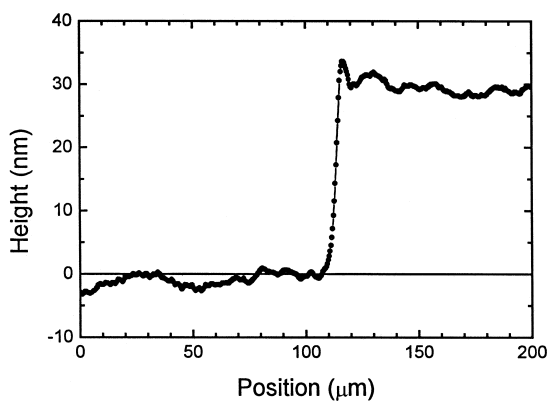

Fig. 4. Profile of the SiO_2 index step, measured with a surface profiler.

Experimentally, the reflectance profiles were determined from surface plasmon microscopy images of the index step. The index step was imaged with both *p*- and *s*-polarized light to correct for inhomogeneities in the incoming beam by dividing the images obtained with the different polarizations. In Fig. 5, the images resulting from resonant plasmons entering the SiO_2 covered area and leaving it again are shown for 11 different wavelengths, with the SPs propagating from left to right. Squares of known size (50 μm) were imaged as well (results not shown), to determine the lateral scale of the images. The reflectance profiles in the direction perpendicular to the index step were determined from the digitized SPM images averaging along the index step.

From these profiles, the periodicity was determined as a function of the wavelength. Eq. (3) shows that this periodicity p is given by

$$p = \frac{2\pi}{\kappa_1' - \kappa_0'}. \tag{7}$$

In Fig. 6, these values are displayed together with theoretical values for a 31.0 nm SiO_2 layer. As this value for d is more accurate than that determined with the surface profiler (and lies within the experimental error of that value), it was used for the calculation of the reflectance profiles.

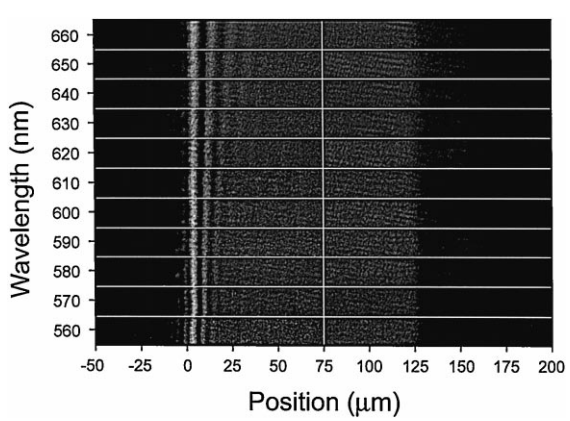

Fig. 5. Composition of all SPM images of the index step, with the resonant plasmon entering (left, at 0 μm) and leaving the cover layer (right, at 125 μm).

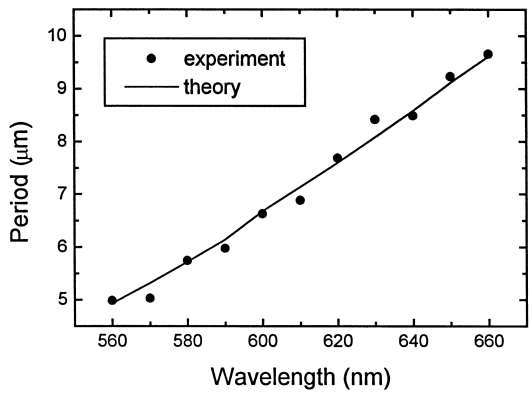

Fig. 6. Periodicity p of the profiles of the images in Fig. 5 as a function of wavelength together with the calculated values for a SiO_2 coverlayer with $d = 31.0$ nm.

These are given in Fig. 7, together with the experimental values. The measured and calculated profiles were normalized by putting the macroscopic values for the reflectance far from the index step to either 0 (at resonance) or 1 (off resonance). The correspondence between experiment and theory is quite good, qualitatively as well as quantitatively. Some fringes to the left of the index step seem to be caused by a reflection that is not accounted for by our or the earlier models [1,2]. They have not always been observed and it is not yet clear how they depend on the exact shape of the index step on a sub-wavelength scale. Therefore, we have left them outside of the scope of the present work. Their dependence on the wavelength is clearly different from that of the fringes on the right of the index step (see Figs. 5 and 7).

5. Conclusion

We have developed a model that describes the reflectance profile in a SPM image near an index step. A silver layer was characterized by fitting

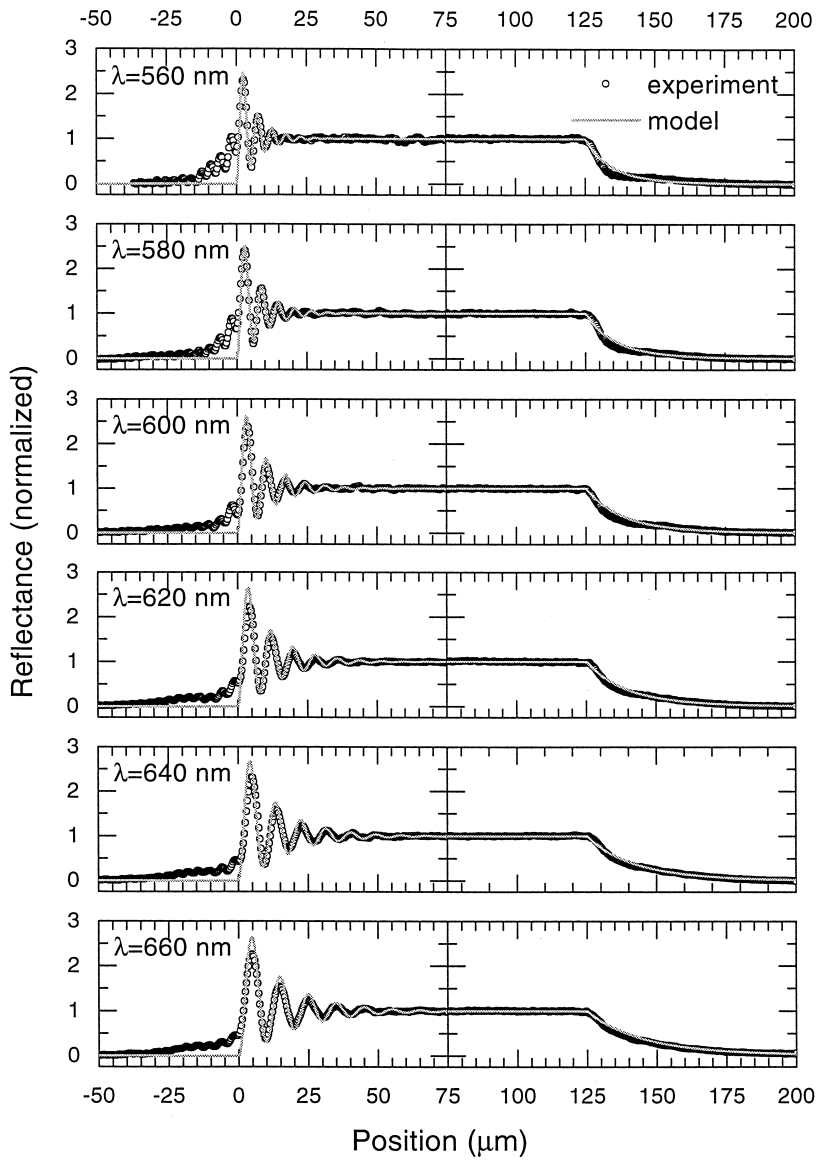

Fig. 7. Calculated and measured reflectance profiles as determined from the images in Fig. 5. The reflectance values at resonance and off resonance were normalized to 0 and 1, respectively.

measured SPR reflectance curves, and the thickness of the cover layer was measured with a surface profiler. Experimental and theoretical values for the reflectance profile as a function of the wavelength were compared and found to agree quite well. Previously, we found similar agreement for measurements on gold [5]. This model can be used to determine which wavelength and metal layer are most suitable for surface plasmon microscopy with a high lateral and thickness resolution.

Acknowledgements

These investigations in the program of the Foundation for Fundamental Research on Matter (FOM)

have been supported (partly) by the Netherlands Technology Foundation (STW).

References

[1] B. Rothenhäusler, W. Knoll, J. Opt. Soc. Am. B 5 (1988) 1401.
[2] B. Rothenhäusler, W. Knoll, Appl. Phys. Lett. 52 (1988) 1554.
[3] T.A. Leskova, N.I. Gapotchenko, Solid State Commun. 53 (1985) 351.
[4] H. Raether, Surface Plasmons on Smooth and Rough Surfaces and on Gratings, Springer-Verlag, Berlin, 1988.
[5] C.E.H. Berger, R.P.H. Kooyman, J. Greve, Rev. Sci. Instrum. 65 (1994) 2829.
[6] W.P. Chen, J.M. Chen, J. Opt. Soc. Am. 71 (1981) 189.
[7] T.J. Watson, J.R. Sambles, Phil. Mag. B 65 (1992) 1141.